Róbert BRÉDA, Tomáš PATZ

Faculty of Aeronautics, Technical University, Košice

Design of measurement chain to measure r.p.m. of an aviation turbo jet engine

Abstract*. The contribution describes the way of improving precision of measuring the revolutions of an aviation turbo-jet engine using a magneto-inductive sensor. Revolutions were evaluated by a specially designed measurement chain making use of optical and inductive sensors. Its core is made up of an Arduino platform with microcontroller ATmega 328P. The object of measurement was an aviation turbo jet engine r.p.m sensor, the DTZ – 2. The results obtained were evaluated in terms of the absolute and relative error. Software developed in the Matlab environment was used for the purpose of on-line plotting of the measured parameters.*

Streszczenie*. W artykule opisano metodę pomiaru prędkości silnika turboodrzutowego, z wykorzystaniem sensora magneto indukcyjnego oraz optycznego. Układ pomiarowy oparto na platformie Arduino z mikrokontrolerem Atmega 328P. Wyznaczono błąd względny i bezwzględny uzyskanych pomiarów. (****Układ pomiaru prędkości obrotowej lotniczego silnika turboodrzutowego****).*

Keywords: r.p.m transmitter, aviation turbojet- engine, measurement chain, optical sensor, inductive sensor, revolutions per minute of the compressor.
Słowa kluczowe: przekaźnik prędkości obrotowej, lotniczy silnik turboodrzutowy, łańcuch pomiarowy, czujnik optyczny, czujnik indukcyjny.

Introduction

The r.p.m of low-pressure and high-pressure parts of the compressor is one of the basic parameters determining the mode of operation for the aviation turbo jet engine. There exist a number of reliable sensors to measure r.p.m, operating on various principles. When starting the crank of the engine, r.p.m is increasing indirectly to fuel injection, temperature and air density, turning acceleration into a rather complicated system. On reducing the throttle, the r.p.m decreases continuously within the entire range of engine modes of operation, making it an unambiguous determinant to the engine operation. The maximum allowable value of the r.p.m depends on: the material used for manufacturing engine blades, forces acting on blades, temperature of the material the blades were made of.

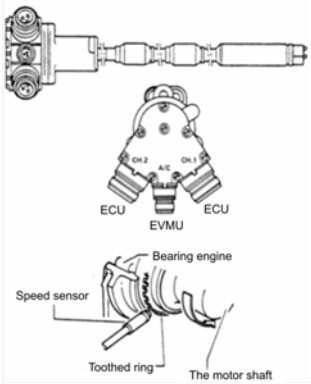

Fig.1 Installation of the N1 inductive sensor of r.p.m an aviation engine.

On aviation turbo-jet engines sensors of r.p.m are installed directly at the low pressure compressor rotor to measure revolutions at the low pressure section and in the casing of driving mechanisms to measure r.p.m of the high pressure compressor section. Transfer of information regarding engine r.p.m in currently used aircraft is substantially different from that of the transfer chains, making use of direct information transfer from the sensor onto the imaging unit, see Fig. 2. Current chains fulfill various functions and are more complex and more complicated [10]. They are able to measure and evaluate vibration and degradation [9, 11, 12]. Fig. 1 illustrates an inductive sensor of a low pressure compressor rotor marked as „N1“ detecting rate of speed of rotation of the rotor within the aviation turbo-jet engine, generating signal for the Engine Vibration Monitoring Unit, the EVMU, and the Electronic Control Unit, the ECU, of the main and back-up channel of the engine control. Currently, there are multiple methods of smart sensor implementation [13] which are based on the standardised solution which does not require too much computational power of the smart sensor system [14].

Structural layout of the object of measurement

In order to improve precision of measuring r.p.m of aviation turbo jet engines under laboratory conditions, a chain of measurement was designed and realized. As a primary sensor to measure r.p.m, a SICK-VTE180-2P41147 opto-electronic sensor and a SICK IM05-0B8NS-ZW1 inductive sensor were used [2, 7, 8]. The object of measurement was a DTZ–2 r.p.m sensor, a standard sensor that measures r.p.m N_1, N_2 of aviation jet engines. The DTZ-2 is an AC generator consisting of a rotor (permanent magneto) rotating inside a slotted stator, witch is connected into the orb by a tree-phase winding. The rotor is of dual-pole design and is cranked by a slotted crank-shaft via a clutch [6]. The generator is attached to the directly to the engine through the case of the driving mechanism Fig. 2. In order to limit the mechanical loading of generators, the operational r.p.m of rotors are reduced applying slow transmission of 2:1 directly from the engine drive.

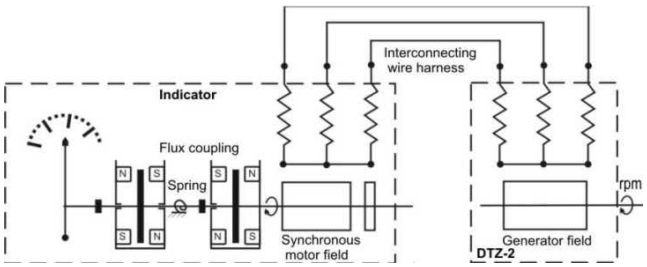

Fig.2. Schematic view of the tachometer system.

At the tachometer system illustrated in Fig. 2, the r.p.m N_1 of the low pressure rotor are from nmax.= 3000 rpm up to 5000 rpm, which represent an error in the precision of measurement from 5 r.p.m to 25 rpm. At the high pressure compressor N_2, the value of rpm falls within the scope of

nmax.=10000 r.p.m as much as 15000 r.p.m, which represents an error in the precision of measurement from 50 r.p.m up to 75 r.p.m.

Designing a measurement chain to measure rpm of an aviation engine

Set-up of the measurement chain to evaluate and improve precision of measuring rpm for aviation engines is made up of from elementary hardware elements: Bolymin BC1602A display [4], Arduino Duemilanov platform with ATmega 328P microcontroller , VTE-180 optical sensor and IM05 inductive sensor, see Fig. 4 [1, 3]. Optical and inductive sensors are powered by 12V DC. To employ optical sensor, it was necessary to construct a visual gauge marker on the mechanical link between the rpm transmitter and the friction clutch, see Fig. 3. Sensing the gauge marker is presented by a pulse on the sensor output. The reference points for the inductive sensor, were determined by the tooth-shape of the flange on the sensor shaft and the clutch.

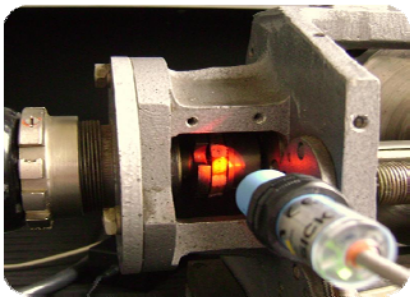

Fig. 3 Installation of the optical sensor and the friction clutch shaft.

Maximal output voltage for processing information from sensors by the micro-checking device was adjusted to the level of 5V. The output information set in this way are then processed by the microcontroller ATmega 328, the task of which was to determine the number of revolutions measured with optical and inductive sensors. The basic element of the program is in its detecting the leading edges of pulses from the sensors for a given time. The program was tested using rotation platform [5].

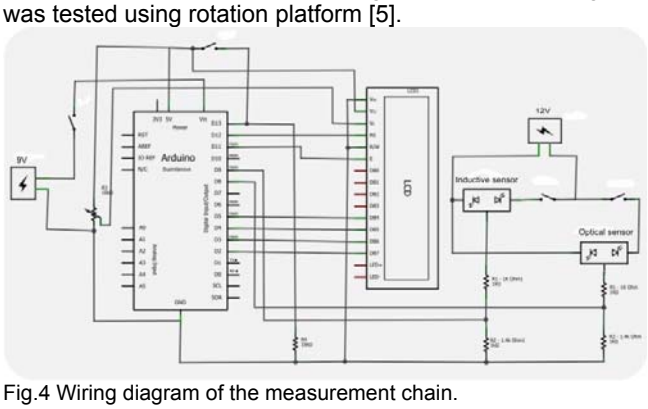

Fig.4 Wiring diagram of the measurement chain.

The developed program converts the rpm, presents it on a display and the measured data are transferred via a series communication into a computer. Precision of the measurement in terms of the frequency of measurement chain was verified by the Agilent LXI 33220A pulse generator. Collection and storage of data in the computer was ensured by series communication. On completion of the measurements, the Matlab performed plotting the final graphical behavior of rpm depending on time.

Experimental verification of sensing the rpm of an aviation engine

Experimental verification of the rpm using the DTZ-2 sensor was performed on equipment designed for measurement of r.p.m of magneto-inductive sensors. The given equipment enables changing revolutions applying an electro-engine and friction clutch, which present the rpm of low pressure turbine of the compressor. Attached to this equipment, via a transmission, are the measured DTZ–2 sensor of rpm and the etalon sensor of rpm, the D–14, see Fig. 5.

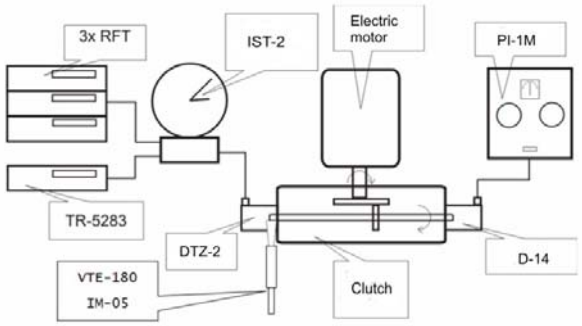

Fig.5 Equipment for measurement sensors of aviation engine rpm.

Connected to the output of the DTZ-2 rpm transmitter output were RFT voltmeters, which served for measurement of voltage of three phases and a counter of pulses a TR-5283, to evaluate the measured frequency. Of the measured parameters, calibration curves **indicators IST – 2 and PI – 1M** for both the optical and the inductive sensor were computed at the known absolute error of 7,5 r.p.m in determining engine revolutions see Fig.6, 7. The value of turbine revolutions in percentages was read also by the couple of electromagnetic indicators of IST–2 and PI–1M.

Table1. Measured parameters using optical sensor

Revolutions [r.p.m]	f_{tr} [Hz]	U_{12} [V]	U_{23} [V]	U_{31} [V]	IST – 2 [%]	PI – 1M [%]
300±7,5 (2,5%)	5	0,97	0,96	0,98	5,8	6
600±7,5 (1,25%)	10	1,90	1,91	1,91	12	12
900±7,5 (0,83%)	15	2,92	2,93	2,93	17,8	18,1
1200±7,5 (0,63%)	20	3,96	3,97	3,97	23,9	24,2
1500±7,5 (0,5%)	25	4,96	4,97	4,99	29,6	30,2
1800±7,5 (0,41%)	30	6,00	6,01	6,02	35,8	36,2
2100±7,5 (0,35%)	35	7,02	7,04	7,05	41,6	42
2400±7,5 (0,36%)	40	8,03	8,05	8,05	46,6	48
2700±7,5 (0,31%)	45	9,05	9,04	9,06	53,9	54
3000±7,5 (0,25%)	50	10,02	10,03	10,05	59,9	60,3
3300±7,5 (0,23%)	56	10,82	10,80	10,83	66,8	67,3
3600±7,5 (0,20%)	60	11,79	11,78	11,80	72	73
3900±7,5 (0,19%)	65	12,83	12,80	12,79	77,7	79
4200±7,5 (0,17%)	70	13,61	13,71	13,68	83,9	84
4500±7,5 (0,16%)	75	14,90	14,94	14,91	90	90
4800±7,5 (0,16%)	81	15,89	15,90	15,92	95,7	97

where: revolutions of the low pressure compressor, (±evaluated absolute error), (relative error), f_{tr} is frequency of the DTZ-2 rpm transmitter output voltage, U_{12}, U_{23}, U_{31} are output interfacial voltages from the DTZ-2 r.p.m transmitter, IST – 2 [%] is percentage presentation of r.p.m from the DTZ – 2 rpm transmitter, PI – 1M [%] is percentage presentation of rpm from the D-24 rpm transmitter.

Table 2. Measured parameters using inductive sensor

Revolutions [r.p.m]	f_{tr} [Hz]	U_{12} [V]	U_{23} [V]	U_{31} [V]	IST – 2 [%]	PI – 1M [%]
300±30 (10%)	5	0,95	0,90	0,93	5,9	6,5
600±30 (5%)	10	1,86	1,87	1,87	11,8	12
900±30 (3,33%)	15	2,82	2,83	2,84	17,7	18
1200±30 (2,5%)	20	3,88	3,88	3,89	24	24,4
1500±30 (2%)	25	4,85	4,86	4,82	29,4	30
1800±30 (1,67%)	30	5,85	5,87	5,88	35,8	36,1
2100±30 (1,49%)	35	6,84	6,83	6,87	41,7	42,2
2400±30 (1,25%)	40	7,93	7,95	7,96	48,2	48,9
2700±30 (1,11%)	45	8,89	8,89	8,81	53,8	54,5
3000±30 (1%)	51	9,86	9,84	9,85	60	60
3300±30 (0,9%)	55	10,74	10,77	10,78	65,7	66
3600±30 (0,83)	60	11,78	11,82	11,80	71,9	72
3900±30 (0,77%)	65	12,90	12,91	12,94	78,1	78,5
4200±30 (0,71%)	70	13,80	13,77	13,79	84	84,5
4500±30 (0,67)	76	14,88	14,87	14,91	90	91
4800±30 (0,625%)	80	15,80	15,79	15,83	95,7	96

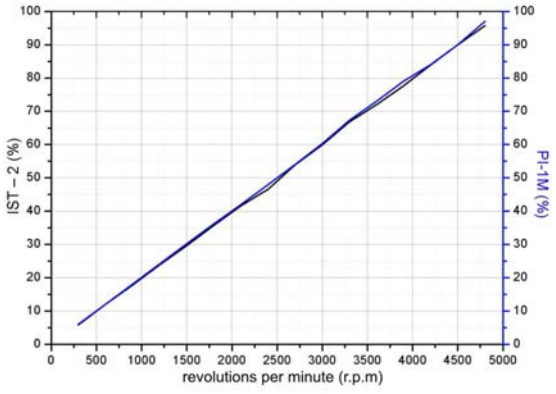

Fig. 6 Calibration curve of IST – 2 and PI – 1M rpm indicators fitted with optical sensor.

Linearity of correction curves was fulfilled up to 99%, as follows from Table 3 by the values of the trend diagram. Based on the calibration curve and expression (1) the revolutions of the compressor *n* were computed from the indicated revolutions N_i.

$$n = \frac{N_i}{b} + a \quad (1)$$

where: n is rpm of low pressure compressor, N_i is rpm indicated, a is beginning (a = 0,082), b is equation line (b = 0,02).

Table 3 Values of the trend slope – optical sensor

Indicator		Amount	Standard deviation
PI-1M	Beginning (a)	-0,0825	0,21479
PI-1M	Slope (b)	0,02015	7,40451E-5
IST – 2	Beginning (a)	-0,285	0,22827
IST – 2	Slope (b)	0,02004	7,86909E-5

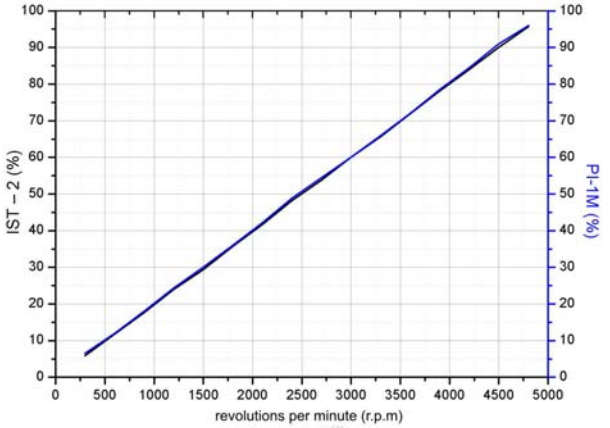

Fig. 7 Calibration curve of IST – 2 and PI – 1M rpm indicators with inductive sensor.

Table 4. Values of trend slope - inductive sensor

Indicator		Amount	Standard deviation
PI-1M	Beginning (a)	0,1575	0,17827
PI-1M	Slope (b)	0,02005	6,14555E-5
IST – 2	Beginning (a)	-0,235	0,10301
IST – 2	Slope (b)	0,02004	3,55099E-5

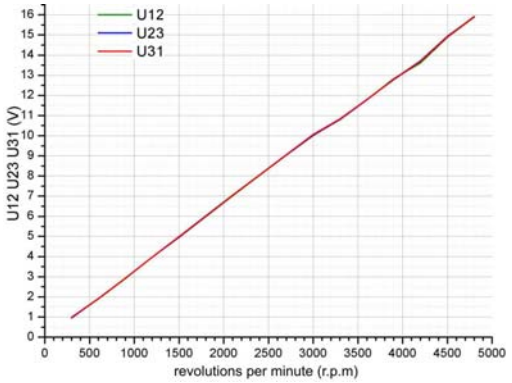

Fig. 8 Behavior of voltage with respect to low pressure compressor rpm, by the designed measurement chain with optical sensor.

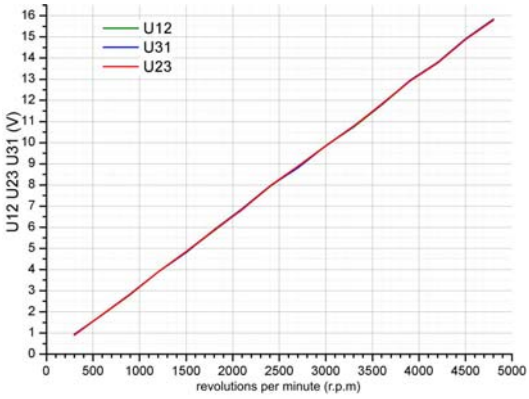

Fig. 9 Behavior of voltage with respect to low pressure compressor revolutions, by the designed measurement chain with inductive sensor.

Based on the measured data, on can determine the revolutions of the low pressure compressor *n* from the value of the output voltage of the DTZ–2 rpm sensor at the known absolute error of 30 rpm in determining revolution of the compressor.

$$n = \frac{U}{b} - a \quad (2)$$

where: n is rpm of low pressure compressor, U is output voltage of the DTZ -2 sensor, *a* is beginning (a = 0,0188), *b* is equation slope (b = 0,00331).
Beginning *a* and of equation slope *b* were obtained from partial data in program OriginPRO 8. When measuring revolution, by means of the optical sensor, the resolution of 7,5 rpm was achieved, which indicates maximal error of ±3,75 r.p.m, when measuring revolutions by means of the inductive sensor, the resolution was 30 r.p.m, which represents the maximal error of ±15 r.p.m.

Conclusion

The designed and realized measurement chain helped achieve improvement in the precision of evaluating the basic measured parameter of the aviation engine - its revolutions. As the object of measurement was the DTZ – 2, a magneto-inductive sensor of aviation engine rpm with remote transmission. Of the measured parameters, determined were the calibration curves of the IST-2 indicator of the measured sensor and the PI-1M indicator of the etalon sensor. Also evaluated were the revolutions of the low pressure compressor by the output voltage of the rpm sensor DTZ-2. For each measurement the error of measurement was evaluated, ± 7,5 r.p.m for the optical sensor and ± 30 r.p.m for the inductive one. For verification of the functionality of connection, check measurements of the aviation engine rpm were performed using the small-size MPM - 20 aviation engine at the specialized facility for controlling intelligent systems, with the test confirming full functionality of the measurement chain.

REFERENCESs

[1] Arduino Hardware, Technical parameters. 2010 <http://arduino.cc/en/Main/arduinoBoardDuemilanove>.

[2] Electric Sensors. Electric Sensors Data and Electric Sensors device: <http://electric-sensors.blogspot.com/2009/04/gear-tooth-hall-effect-speed-sensor.html>.

[3] Kosaka, Kimio : Burningthe Bootloader without external AVR writer:<http://www.geocities.jp/arduino_diecimila/bootloader/index_en.html>.

[4] LCD MODULE SPECIFICATION, MODULE NO. BC 1602E series.<http://www.soselectronic.ro/a_info/resource/d/bolymin/BC1602E_Series_VER01.pdf>.

[5] Sotak M.: Testing the Coarse Alignment Algorithm Using Rotation Platform, In: Acta Polytechnica Hungarica, Vol. 7, No. 5 (2010), , p. 87-107, ISSN 1785-8860

[6] Pallet E.H.J.: Aircraftinstruments and integratedsystems , Harlow, 1992.

[7] SICK. V180 M18 Cylindrical photoelectric sensorseries, Datasheet, 2010 . : <http://www.sensorica.ru/pdf/V180-2.pdf>.

[8] SICK. IM 05 Cylindrical inductive sensorseries , Datasheet 2010,<http://www.sick automation.ru/images/File/pdf/DIV01/im05.pdf>.

[9] Sotak, M.: Determining stochastic parameters using an unified method. In: Acta Electrotechnica et Informatica. - ISSN 1335-8243, Vol. 9, No. 2 (2009), p. 59-63.

[10] Dub, M.; Jalovecký, R.: Rotational Speed Signal Digitizing. In Zborník príspevkov z medzinárodnej vedeckej konferencie "Nové smery v spracování signálov VIII". May 24-26, 2006, Tatranské Zruby, Slovak Republic. Liptovský Mikuláš : Akadémia ozbrojených síl generála Milana Rastislava Štefánika, 2006, s. 90-94. ISBN 80-8040-294-9.

[11] Kuffová, M.; Soták, M.: Simulation techniques for evaluation degradation processes: monograph, 1. ed., Liptovský Mikuláš, Armed Forces Academy, 2010, ISBN 978-80-8040-414-7. (in Slovak)

[12] Roháč, J.; Reinštein, M.; Draxler, K.: Data Processing of Inertial Sensors in Strong-Vibration Environment. In Intelligent Data Acquisition and Advanced Computing Systems (IDAACS). Piscataway: IEEE, 2011, vol. 1, p. 71-75. ISBN 978-1-4577-1426-9.

[13] Pačes, P.; Reinštein, M.; Draxler, K.: Fusion of Smart Sensor Standards and Sensors with Self-Validating Abilities In: Journal of Aircraft. 2010, vol. 47, no. 3, p. 1041-1046.

[14] Popelka, J.; Pačes, P.: Performance of smart sensors standards for aerospace applications. Przeglad Elektrotechniczny. 2012, vol. 88, no. 01a, p. 229-232. ISSN 0033-2097.

***Authors**: Ing. PhD. Róbert Bréda, Technical university Košice, Faculty of Aeronautics, Department of Avionics, Rampová 7, 04021 Košice, Slovakia, E-mail: robert.breda@tuke.sk*
Ing. Tomáš Patz, Technical university Košice, Faculty of Aeronautics, Department of Avionics, Rampová 7, 04021 Košice, Slovakia, E-mail: tomas.patz@gmail.com